

# Predicting synchronous firing of large neural populations from sequential recordings

Oleksandr Sorochynskyi,<sup>1</sup> Stéphane Deny,<sup>2</sup> Olivier Marre,<sup>1,3</sup> and Ulisse Ferrari<sup>1,3</sup>

<sup>1</sup>*Sorbonne Université, INSERM, CNRS,*

*Institut de la Vision, 17 rue Moreau, 75012 Paris, France.*

<sup>2</sup>*Neural Dynamics and Computation Lab, Stanford University, California*

<sup>3</sup>*Equal contribution*

## Abstract

A major goal in neuroscience is to understand how populations of neurons code for stimuli or actions. While the number of neurons that can be recorded simultaneously is increasing at a fast pace, in most cases these recordings cannot access a complete population: some neurons that carry relevant information remain unrecorded. In particular, it is hard to simultaneously record all the neurons of the same type in a given area. Recent progress have made possible to profile each recorded neuron in a given area thanks to genetic and physiological tools, and to pool together recordings from neurons of the same type across different experimental sessions. However, it is unclear how to infer the activity of a full population of neurons of the same type from these sequential recordings. Neural networks exhibit collective behaviour, e.g. noise correlations and synchronous activity, that are not directly captured by a conditionally-independent model that would just put together the spike trains from sequential recordings. Here we show that we can infer the activity of a full population of retina ganglion cells from sequential recordings, using a novel method based on copula distributions and maximum entropy modeling. From just the spiking response of each ganglion cell to a repeated stimulus, and a few pairwise recordings, we could predict the noise correlations using copulas, and then the full activity of a large population of ganglion cells of the same type using maximum entropy modeling. Remarkably, we could generalize to predict the population responses to different stimuli and even to different experiments. We could therefore use our method to construct a very large population merging cells' responses from different experiments. We predicted synchronous activity accurately and showed it grew substantially with the number of neurons. This approach is a promising way to infer population activity from sequential recordings in sensory areas.

## Introduction

A major goal of neuroscience is to understand how populations of neurons process sensory stimuli. This understanding is limited because, among other reasons, accessing the activity of all neurons of a sensory structure is very challenging. Most techniques only give access to a small fraction of neurons [1, 2] (but see [3, 4]), leaving as hidden variables many neurons that may play a role in information processing but are not recorded.

To overcome this issue, an emerging, ‘divide and conquer’ approach is to first classify the neurons in a given area into different cell types, where neurons of the same type are supposed to be functionally identical. Then, in a second step, one can characterize the neuronal function of each cell type, to eventually predict how populations composed of all the neurons of the same type will respond to sensory stimuli.

There has been tremendous progress recently in achieving the first step of this approach. Several studies have shown that it is possible to cluster cells in different homogeneous types [5]. This can be done using either the responses of each cell to several standard stimuli [6–8], or using genetic tools [9, 10]. These methods have proven successful in isolating most cell types in the retina [7, 11, 12] and there are several ongoing studies trying to apply these approaches in the cortex [13].

For the second step, many studies have tried to model and predict how neurons of a single type respond to complex stimuli. This strategy has been applied in the retina [14–18] and in many low-level areas [19–21]. A complementary strategy is to use mouse lines expressing GFP in specific cell types in order to record sequentially (i.e. repeatedly across different experiments) from cells that are functionally identical. This has been performed in the retina [6, 22] and enables one to present as many stimuli as desired to cells belonging to the same type. It is thus possible to gather a lot of information about how single neurons of a well-defined cell type will respond to many different sensory stimuli, using sequential recordings of neurons of the same type taken from different experiments.

Extensive characterization of single cell responses to sensory stimuli is thus possible. The next challenge is to infer how the entire ensemble of neurons of a single type responds together to stimuli. Ideally, one would like to record from all the neurons of a given type, but this is rarely possible.

One possible strategy is to use these sequential recordings from cells of the same type to reconstruct how the entire population will respond. However, reconstructing the activity of a full population from sequential recordings cannot be done by simply pooling the responses to a given stimulus from many sequential recordings. In many cases, pairs of neurons are correlated due to shared noise (noise correlation), which might significantly reshape the neurons’ activity [23], and play an important role in information encoding and transmission [15, 24–29]. Because these noise correlations cannot be predicted from sequential recordings, a model is needed to predict them and therefore to infer the activity of a full population of neurons of the same type.

Previous works have tried to model and predict the activity of ensembles of neurons in the retina [15, 30–33]. However, they were fitted and tested on ensemble of neurons recorded simultaneously, and it is unclear if they can generalize to predict correlated activity across experiments, a critical feature necessary to reconstruct activity from sequential recordings. Overall firing rates will vary between experiments, and this variation will make these models unlikely to predict noise correlations across experiments.

Here we address this issue and propose a method to infer the activity of an entire population of neurons of the same type from sequential recordings in the retina. Our method assumes that we have access to many single cell recordings gathered from different experiments of neurons of the same type, where the same stimulus has been displayed, and additionally to a few recordings of pairs of neurons of the same type. We used these data to reconstruct the activity of a large population of neurons, with a shared noise consistent with the paired recordings.

We applied this method in the rat retina, where the activity of many neurons of the same type can be recorded through repetitions of multi-electrode array experiments [3], so that the method can be validated. We first show that a copula-based analysis [34–37] of synchronous activity allows a simple description of noise correlations, that is invariant across stimulus identities and experimental preparations. This description depends only on the individual activities of pairs of cells and on their physical distance. This result allowed us constructing a model based on copulas and to predict -across experiments- the extent of pairwise noise correlations from sequential recordings of neurons of the same type. From this estimation of pairwise correlations we then used a time-dependent maximum entropy model [31–33] to infer the activity of the full population of neurons of the same type. We show that this method is accurate and reproduces several features of the recorded population activity. We then applied our method to infer the activity of a large population of neurons of the same type, beyond what can be currently recorded experimentally. Thanks to our inference method, we could estimate the extent of synchronous firing in such a large population, and show that it grows significantly for large populations.

As soon as sequential recordings of many cells of the same type will be available also in cortical systems, it will be possible to apply our method to reconstruct the activity of large populations even beyond the retina.

## Results

### Overview of the inference method

The purpose of our method is to reconstruct the activity of a population of neurons of the same type from their individual responses to a same stimulus. Part of this population activity is directly accessible from sequential recordings, but another part needs to be predicted. For example, if we have recorded sequentially two neurons responding to the same stimulus, a naive solution is to pool together their responses as if they had been recorded at the same time. If the noise present in these responses is independent between the two neurons, this is indeed equivalent to record them together. However, in many cases, the noise between different neurons is correlated. In that case, pooled sequential recordings are not equivalent to simultaneous recordings [23], and the difference is what is usually termed the noise correlation between these two neurons.

Our method aims at inferring these noise correlations from parsimonious pairwise recordings of a few cells, and use them to predict how noise will be correlated across an entire population of hundreds of neurons. From this we can reconstruct how a large population of neurons would respond if they were recorded simultaneously, based on sequential recordings.

Our method is divided in three steps. First, we infer the parameter of a model based on copulas [34–36] from simultaneous recordings of few cells. Second, we used the inferred model to predict noise correlations between pairs of neurons from sequential recordings, using only information on the distance between the recorded cells. Our method allows predicting noise correlations for the same pair of neurons responding to a different type of stimulus, and can generalize to predict noise correlations for another pair of neurons of the same type recorded in a different experiment. Third, we use a time-dependent maximum entropy model [31–33] to generalize from pairs of neurons to a full population. This step does not require any additional empirical information with respect to the second step. Note that simultaneous recordings are necessary only for model inference (and validation), yet sequential recording are sufficient for making prediction.

Here we applied this method to cells of the same type in the rat retina. These data allowed us testing if our reconstruction of the population activity is accurate. Finally, we used our method to infer the synchronous activity of a large neuronal population, much larger than what is nowadays experimentally accessible.

### Strong noise correlations between nearby OFF retinal ganglion cells.

We recorded rat retinal ganglion cells (RGCs) in response to different visual stimuli. We used a previously described method [18] to divide them in different types. Briefly, we clustered their responses to a full field flicker and isolated a single type of OFF-alpha ganglion cells. All these cells responded reliably to a checkerboard stimulus (Fig. 1A). The cell responses to random checkerboard have been used to estimate their receptive fields and to find their location. The receptive fields of these cells tiled regularly the visual field (mosaic in Fig. 1B).

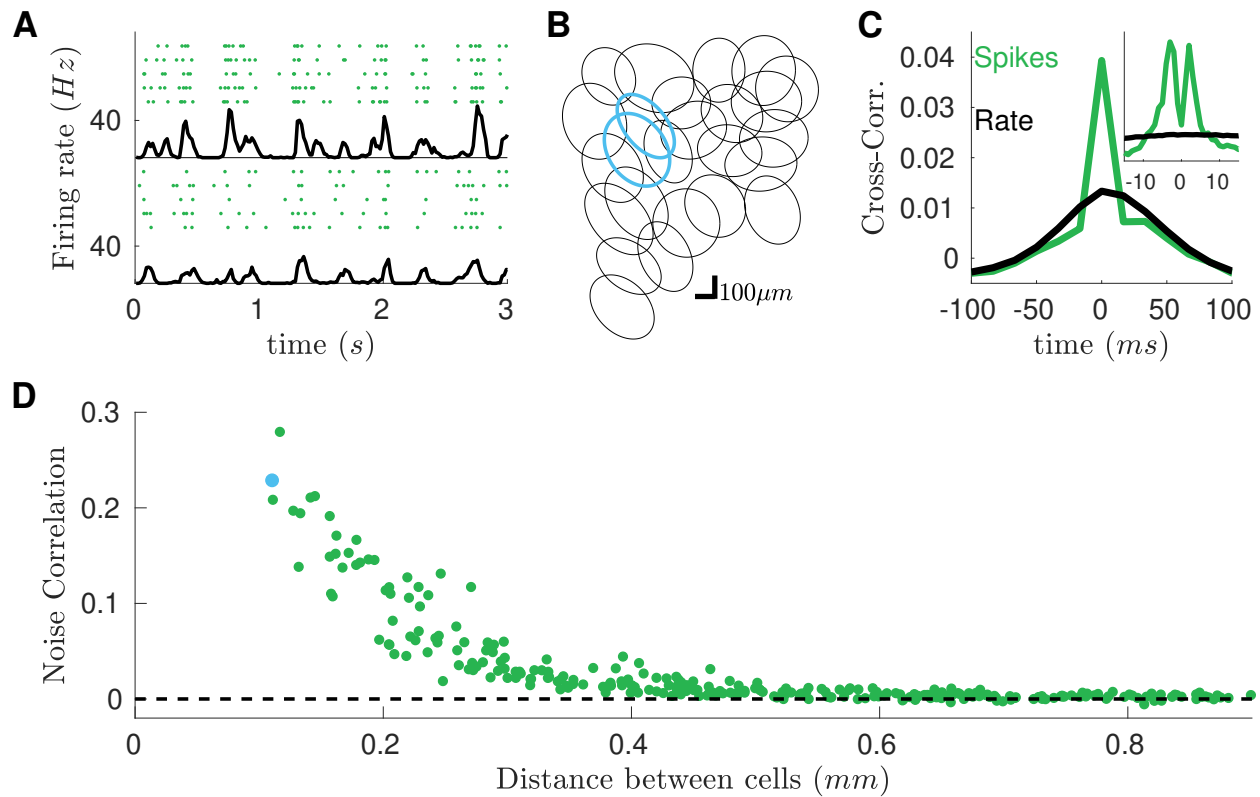


**FIG. 1: High noise correlation between nearby RGCs subject to checkerboard stimulation.** **A)** Raster plots of two example cells in response to checkerboard stimulation. Each line corresponds to a repetition of the same visual stimulation. Black line: averaged firing rate of the cell. **B)** Receptive field mosaic of the recorded OFF cell population. Cyan receptive fields refer to the cells showed in panel A. **C)** Cross-correlation for the two cyan cells (green,  $dt = 17ms$ ), superimposed to the cross-correlation of their firing rates (black). Inset: Cross-correlation at finer time scales ( $dt = 1ms$ ). **D)** Zero-lag ( $dt = 17ms$ ) noise-correlation plotted against the distant between cells.

To estimate noise correlation between pairs of cells, we computed the cross-correlation of their spike count and the cross-correlation of their firing rate (the mean over stimulus repetitions of the spike count, respectively green and black lines in Fig. 1C inset). At short time-scales, spike-count correlation is larger than that of firing rates, but only for nearby pair of cells (see Fig. 1C). We term noise-correlation the difference between the zero-lag cross-correlation of spike counts and firing rate (see Methods). We observed a similar behavior for all visual stimulations and experiments.

In the following we used these data to test our method. We first used copulas to predict the noise correlations between pairs of cells. We then used maximum entropy model to reconstruct the activity of a large population of ganglion cells from sequential recordings.

## Copula model predicts pairwise response from sequential recordings.

121

A copula is a method to build pairwise probability distributions from pairs of single-variable distributions (see Fig. 2 and Methods). We used this approach to build the joint spike count distribution of pairs of neurons, that, if marginalized, reproduces the empirical single neuron distributions. For each time-bin, for each recorded neuron, we first estimated the distribution of spike count from its response to stimulus repetitions, and from this we obtained its cumulative distribution function. Next, for each pair of neurons, we fitted one copula distribution to the collection of joint cumulative functions of activity. We then drew samples from the inferred copula distribution, i.e. pairs of real numbers between 0 and 1 ( $(u_1, u_2) \in [0, 1]^2$ ) with uniform marginal distribution. Finally, we used the inverse the cumulative distribution functions to transform these samples into pair of integers, which followed the predicted joint spike-count distribution.

122  
123  
124  
125  
126  
127  
128  
129  
130  
131  
132

A copula is characterized by a parameter that tunes the interaction strength of the two variables, and that can be inferred from data. We found that this copula parameter only depended on the distance between the two cells, and can be fitted using a function with just three parameters ( $\theta = \exp(a + bx + cx^2)$ , where  $x$  is the distance between the two cells, see Fig. 2B, suppl. sect. S2 and Fig. S1). We could thus describe the joint activity between all pair of neurons using copulas characterized by only three parameters across the entire population of cells. Once applied on the same response to checkerboard stimulation used for training, our model predicted noise correlations with high accuracy (Pearson's  $\rho = 0.99$ ,  $n = 300$  pairs, larger than  $\rho = 0.92$  obtained by fitting directly noise correlations, see supplementary sect. S3).

133  
134  
135  
136  
137  
138  
139  
140  
141  
142

We have built a model with only 3 parameters, that can predict the noise correlation between any pair of neurons from the activity of single cells. We then tested if this model can generalize and predict noise correlations measured in response to different stimuli. We first inferred the copula model from the response to checkerboard stimulation (that of Fig. 1). Then, from the response to repetitions of another type of stimulus, we estimated the spike-count distributions of each neuron in each time-bin. Finally, we used our copula model to first build the joint distribution, and then compute the mean noise-correlations of each neuron pair. We applied this strategy to the RGCs' response to full-field and moving-bar stimuli, see Fig. 2. In both cases, the copula model was able to reproduce the empirical estimates of noise-correlations with high accuracy (Pearson's  $\rho = 0.96$  for full-field and  $\rho = 0.97$  for moving-bar,  $n = 300$  pairs).

143  
144  
145  
146  
147  
148  
149  
150  
151  
152  
153

To further demonstrate the robustness of our method we tested if our copula model could predict noise correlations in a different RGC population of the same type, recorded in a different experimental preparation. We used the model inferred from the data of the first experiment to predict noise correlations between the same type of RGC, but recorded during a second experiment. Using only single cell responses, our model predictions were accurate (Fig. 3B, Pearson's  $\rho = 0.96$ ,  $n = 496$  pairs), and accounted for how noise correlations decrease with distance (Fig. 3C). The functional dependence of the copula parameter with respect to inter-cell distances is thus robust across experiments, and hence corresponds to a general property of OFF-Alpha cells in the rat retina. We obtained similar results for all the 8 testing experiments (averaged Pearson's  $\rho = 0.949 \pm 0.017$ , for a total of  $n = 1632$  pairs).

154  
155  
156  
157  
158  
159  
160  
161  
162  
163

Note that in order to predict noise correlations (Fig. 3) our model never accessed to the simultaneous recordings, but only to the collection of single neuron responses. We could

164  
165

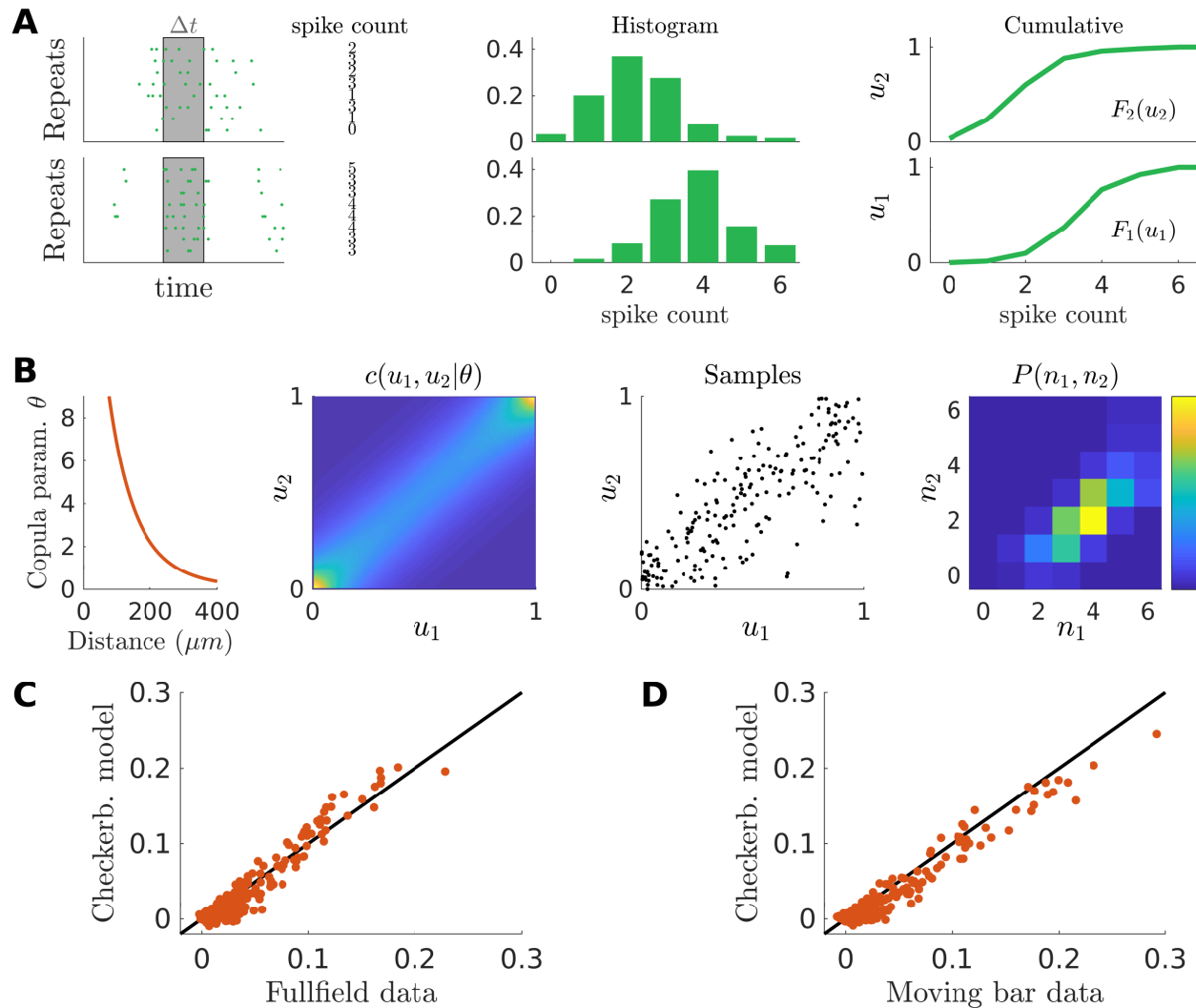


**FIG. 2: Copula model predicts noise correlations across stimulus ensembles.** **A)** Illustration of our copula model: first step. Spike counts are estimated across stimulus repetition for a given pair of cells, in a given time-bin. Empirical histogram of the spike counts are then estimated and later used to compute the empirical cumulative distribution function. **B)** Second step. A parametric function allows to estimate the copula parameter  $\theta$  as a function of the cells' distance. A copula distribution then accounts for the mutual dependency of two random variables. From it we draw many samples of pairs of real numbers  $(u_1, u_2) \in [0, 1]^2$  with uniform marginals. Inverse of the cumulative distribution functions transform these samples into pairs of positive integer numbers, whose distribution matches the empirical spike count marginals by construction and accounts for their mutual dependency. **C)** Scatterplot of the empirical and model predicted noise correlations from the response to full-field stimulation. **D)** As **C)** but for the moving-bar stimulation. In both case the model has been inferred from the response to checkerboard stimulation.

have thus predicted the noise correlation between pairs of neurons in these new experiments using only the sequential recording of each neuron. Our approach thus allows predicting

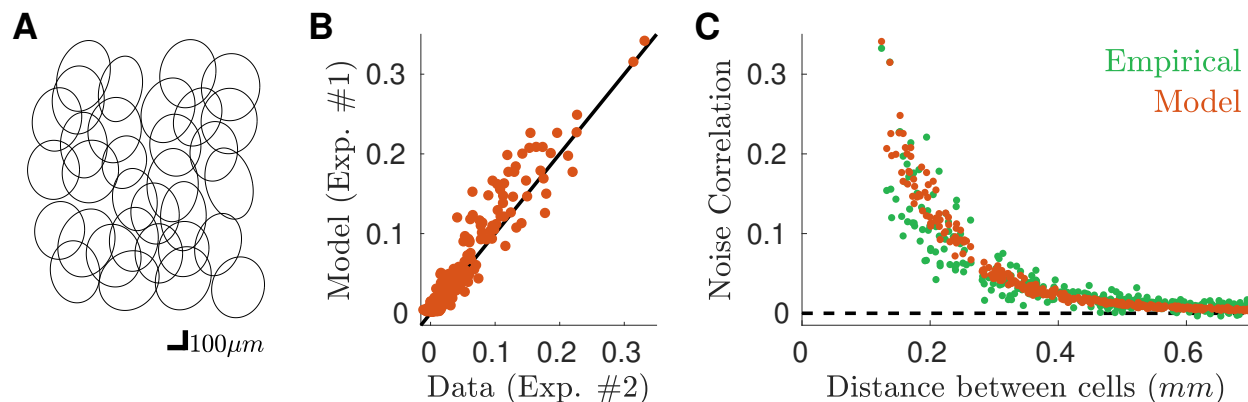


**FIG. 3: Copula model predicts noise correlations across experimental preparations.** **A)** Receptive field mosaic of the recorded OFF cell population for a new dataset, different from the one used for training the model. **B)** Scatterplot of the empirical and model predicted noise correlations from the response to checkerboard stimulation. **C)** Behavior of the empirical and model predicted noise correlations plotted against the distance between cells. Data from a second dataset (#2), different from the one used for training the model (#1).

pairwise noise correlations across experiments without requiring simultaneous recordings. 168

### Time-dependent maximum entropy model reconstructs the activity of large population from the copula's pairwise predictions. 169 170

Our copula model predicted pairwise synchronous firing. To reconstruct the activity of a large population of neurons from single cell recordings, we then used a *time-dependent* Maximum Entropy population model. 171  
172  
173

Standard Maximum Entropy models [30] aim at predicting the probability of any spike pattern from the mean firing rate of each neuron and the correlations between each pair of cells. Here we use a recent generalization of this approach [32, 33] that takes into account a time-varying firing rate. This approach built a collection of pairwise Maximum Entropy models (one for each time-bin), which share the same couplings, but with different external inputs (fields) for each cell and each time bin [32, 33] (see Methods). *Time-dependent* Maximum Entropy modelling thus disentangles intrinsic interaction, due to network effects, from extrinsic correlations, due to common inputs [33]. 174  
175  
176  
177  
178  
179  
180  
181

We inferred the *time-dependent* Maximum Entropy population model from the activity of single neurons and the pairwise correlations predicted by the copula model. The inferred couplings are large only between nearby cells, see Fig. 4A, and the model reconstructs a “nearest-neighbor” interaction network, see Fig. 4B. As expected the model reproduced well the pairwise noise correlation (Fig. 4C, Pearson’s  $\rho = 0.96$ ,  $n = 496$  pairs), which were already finely predicted by the copula model (Fig. 3B). Remarkably, Fig. 4D shows that the model also accounts for the triplet noise correlation (see Methods) (Pearson’s  $\rho = 0.6$ ,  $n = 4960$  triplets). In order to show that our model captures the synchronous behavior of the neuronal population, we compute the probability distribution of the population rate, i.e. the 182  
183  
184  
185  
186  
187  
188  
189  
190



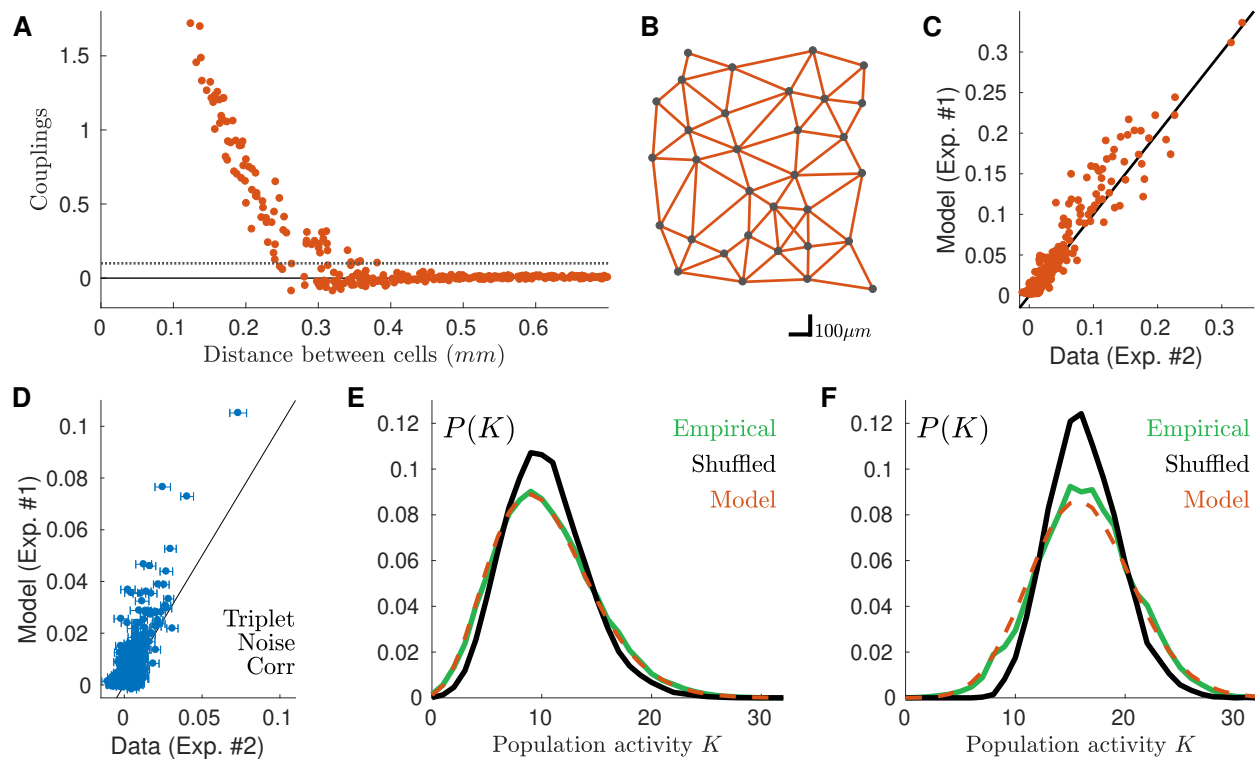


**FIG. 4: Time-dependent Maximum Entropy model predicts population synchronous firing across experimental preparations.** **A)** Behavior of the inferred couplings with the distance between cells. Grey dotted line threshold for identifying strong couplings (see panel **B**). **B)** Position of the cells on the retinal surface, and strong couplings linking them. In the model, only nearest neighbor cells are directly interacting **C)** Noise correlation prediction of the model against empirical value. As expected by construction, the model reproduces the copula estimations, and hence the empirical values (see Fig. 3B). **D)** Model prediction of triplet noise correlations against empirical value (Pearson correlation  $\simeq 0.6$ ,  $n = 4960$ ). **E)** Empirical, shuffled (cond. independent) and model distributions of the population activity averaged over all time-bins. **F)** Same as **E** but for the 5% of time-bins with the highest mean population firing rate. Data from a second dataset (**#2**), different from the one used for training the model (**#1**).

total number of spikes emitted by the entire population in a given time-bin. We compared this distribution with the “shuffled” distribution, which destroys noise correlations, and is equivalent to the prediction made by a conditionally-independent model (i.e. a model that would assume there are no noise correlations). The distribution computed after shuffling the data overestimated the probability of number of spikes close to the average population rate, and underestimated the occurrence of transients of very large or very low activity (see Fig. 4E and F). Remarkably, our model captured the empirical behavior of the population rate averaged over the whole recording (see Fig. 4E). It also performed well when focusing only on highly active time-bins (Fig. 4F).

191  
192  
193  
194  
195  
196  
197  
198  
199

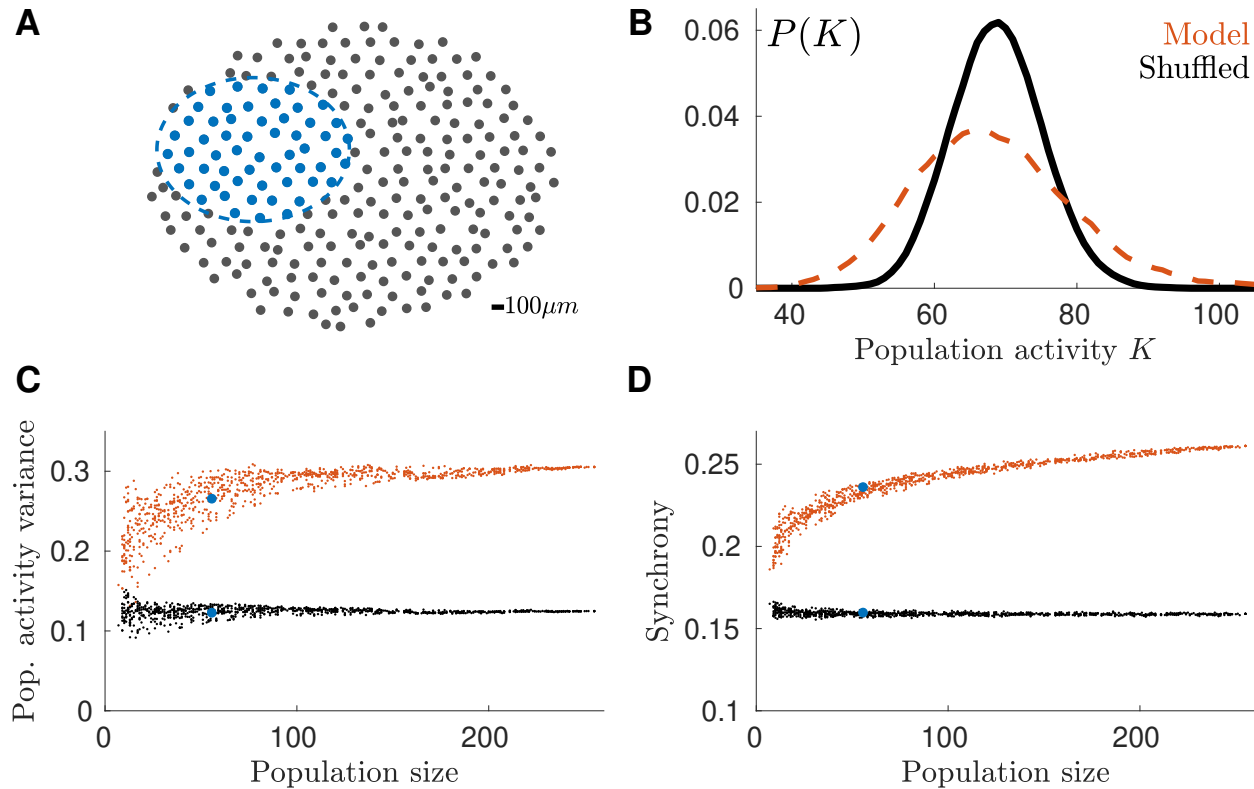


FIG. 5: **Large population model.** A) Synthetic mosaic of  $n = 256$  cells. Blue: example of sub-population. B) Probability distribution of the population activity for the time-bin with the highest firing rate. C) Average over time of the population activity variance for many sub-populations. D) Behavior of Synchrony with the number of cell in the sub-population.

### High synchrony in a large population of ganglion cells reconstructed from multiple experiments

Thanks to our model, we could reconstruct the activity of a large population of neurons using only single cell activity. Since the model can generalize across experiments, it means that the activity of the different single cells can be taken from different experiments. Our method only needs a few pairs of neurons recorded simultaneously to fit the three parameters of the model. In the following we illustrate how this model can be used to reconstruct the activity from a very large population of neurons, bigger than what could be recorded experimentally. We illustrate how this inference of the activity of a large population of cells can be useful by measuring synchronous activity over increasing number of cells.

We collected the (marginal) response of many cells recorded during multiple experiments, and constructed a large population of  $n = 256$  cells. We first built a synthetic lattice representing the positions of the cells reproducing the empirical statistics of inter-cells distances (Fig. 5A and Methods). Then, we associated to each lattice position the response to the checkerboard stimulus of a randomly chosen cell among the ones recorded in all experiments (excluding those from the experiment used to learn the model parameters). Finally we applied our two-step approach to predict how this large population of cell would have responded

to a checkerboard stimulus. 218

At first, we looked at the population rate as previously defined. In comparison with shuffled data, our model predicted a more frequent occurrence of transients with either very high or very low population activity (Fig. 5B). This is a signature that synchronous activity extends up to large populations. To study how correlated firing grows with the population size, we sub-sampled the synthetic model (Fig. 5A) and computed the variance of the population rate. The variance predicted by the model grows with the number of neurons (Fig. 5C) and saturates at  $\sim 200$  neurons ( population activity variance is  $0.24 \pm 0.02$  at  $N \simeq 30$  cells and  $0.299 \pm 0.002$  at  $N \simeq 200$  cells , mean  $\pm$  s.d.), much larger than the typical number of cells recorded in an experimental session. On the contrary, in the reshuffled control, the variance is smaller and roughly constant when the number of neurons increases. Next we estimated the synchrony in the population as the probability of observing a transient with large population activity (see Methods). This synchrony grew fast for small number of cells and stopped increasing at  $\sim 200$  cells ( synchrony is  $0.221 \pm 0.004$  at  $N \simeq 30$  cells and  $0.257 \pm 0.001$  at  $N \simeq 200$  cells , mean  $\pm$  s.d., Fig. 5D) . 219  
220  
221  
222  
223  
224  
225  
226  
227  
228  
229  
230  
231  
232

## Discussion

233

We have shown that our new method allows for reconstructing the population activity of large populations of neurons of the same type in the retina, based on sequential recordings and a few pairwise recordings. We have first developed a model to predict noise correlations across experiments. Thanks to this, once the model parameters are learned with paired recordings, we can take any pair of cells taken from new experiments, and predict the noise correlations from the activity of each single cell. Thanks to this prediction we could then reconstruct the activity of large populations of neurons of a single type at a scale beyond what can be recorded experimentally. Using this method, we have shown that synchrony in the population of OFF-alpha ganglion cells grows with the number of cells, and become large for large populations. Understanding how the collective behaviour of neural ensembles scales with the number of neurons is a crucial issue, and our tool is a key method for this purpose, because it allows accurate inference of population activity, at a scale currently not accessible with experimental recordings.

234  
235  
236  
237  
238  
239  
240  
241  
242  
243  
244  
245  
246

Previous works have shown how different methods can be used to model and predict noise correlations. The Generalised Linear Model [15] uses spike history filters to couple the spiking activity between different neurons. Stimulus dependent maximum entropy models [32, 33] have coupling terms to model synchronous activity between pairs of neurons. These models have been successfully used to model how a population of neurons responds to a stimulus ensemble. However, they usually fail in trying to predict the population activity in responses to different stimuli. This is because the parameters generating the correlations usually change when learned on different stimulus statistics [38]. Moreover, they were never used to predict the activity of a population across different experiments. A main obstacle for this is that firing rates can vary from experiments to experiments, which would induce parameter changes in most of these models, and make generalization difficult. Here we have found that the noise correlation could be predicted using our model knowing just the distance between the two cells and their individual activity. We could then predict noise correlations across experiments. Having a model that generalizes across experiments is crucial to pool together recordings from neurons of the same type and reconstruct activity of large neural ensembles.

247  
248  
249  
250  
251  
252  
253  
254  
255  
256  
257  
258  
259  
260  
261  
262

Our ability to generalize across stimuli and even experiments demonstrates that the couplings between the recorded ganglion cells are insensitive to the context. This means that these couplings reflect an intrinsic property of the retinal circuit, and that the mechanism generating these noise correlations is not influenced by changes in the stimulus or in overall firing rate. Since the timescale of the observed noise correlations is very fast (few ms), the most likely mechanism is gap junctions, which create direct electrical connections between ganglion cells [39]. Noise correlations might be more dependent on the context if they are generated by a shared noise source, e.g. the photoreceptor noise [40]. Nevertheless, our results suggest that the strength of gap junctions are tuned to a value that seems preserved between different experiments.

263  
264  
265  
266  
267  
268  
269  
270  
271  
272

Our approach to model noise correlations is based on copula distributions, and assumes that the copula parameter is constant across experiments. An alternative, simpler approach could have been to assume that noise correlations themselves remain similar across experiments. We constructed this simpler model by fitting an exponential function over noise correlations in our training dataset. This approach, however, gave significantly worse results

273  
274  
275  
276  
277

than our method based on copulas (see supplementary sect. S3), demonstrating that our approach captures non-trivial properties of the correlated firing, i.e. its dependence on the firing rate of each cell.

Remarkably, our description of noise correlation depends only on the physical distance between the pair (see supplementary sect. S2). We have relaxed these assumptions and found that the copula parameter did not vary much with time, cell identity or stimulus. First, if we assume one copula parameter per time bin for a given pair of neurons, it varied little with time, and approached a constant value when the pairs' firing rate were large enough (see supplementary Fig. S1A and B). Second, when we inferred one parameter for each pair of cells to account for cell identities, their values still followed closely our parametric function (see supplementary Fig. S1C). Finally, when we inferred copula parameters from the response to different stimulus ensembles, we obtained very similar values (see supplementary Fig. S1D). This shows that the same copula distribution accounts well for the correlation between the two cells, independently of their firing rate, identities and of the stimulus ensemble.

Copulas have rarely been used in neuroscience studies [35–37, 41–43], but none of them applied this method to predict noise correlations. In [35], Pillow and co-workers proposed for the first time discrete copula distributions to model the total spike-count correlation in pre-motor cortex neurons. However, they did not distinguish stimulus from noise correlations as we have done here.

An interesting outcome of our method is the possibility to construct models of arbitrary large populations, as long as enough sequential recordings are available. This possibility opens for testing a number of hypotheses on how correlated firing affects the overall population activity. Previous studies [30, 44] have made conjectures on the behavior of the retinal synchronous activity at large scale by extrapolating their results from the smaller number of cells experimentally available. The validity of these extrapolations has been recently questioned [45], pointing out how the observed correlation pattern of small systems must be different from that of larger ones. Here we build a large population model (Fig. 5) pooling together real data and using our validated model to infer noise correlations between cells. Our synthetic model thus provide the framework to further test the conjectures on the system' behavior for large numbers of neurons, beyond what can be done experimentally.

Our approach is general and could be applied in any sensory area, provided that sequential recordings of the same type of cells are available, as well as some pairwise recordings to fit the model parameters. We applied it in the retina, where it is possible to have recordings of many neurons of the same type. We could thus validate our method and show that excess synchrony (i.e. beyond what could be predicted by a conditionally-independent model) increased with the number of neurons, and becomes more and more significant at larger population sizes. Recent technological advances will make this method relevant to understand cortical populations, where it should be soon possible to define the cell type of each recorded cell using genetic (e.g. single cell transcriptomics [9, 10]) and physiological (e.g. clustering of responses [7]) tools. One issue could arise if noise correlations strongly depend on the stimulus, as it has, for example, been reported for V1 [46]. In our data, noise correlations depend very little on the stimulus, which allowed us to reduce our model and let copula parameters depend only on the distance between cells. However, if noise correlations depend largely on the stimulus, the model can be extended. The simplest solution would be to make the copula parameters depend on the stimulus. If this stimulus dependence can be explicitly modeled, our method would still manage to predict the activity of large ensembles

of neurons. 324

Finally, here we predicted the responses of a population of neurons to a stimulus for which 325  
we have access to single cell responses across stimulus repetitions. If a model is available to 326  
predict the responses of single cell to other stimuli, it could be used to predict the marginal 327  
probability distribution of each individual neuron, and then combined with our approach 328  
to predict the activity of the whole population. This makes our method complementary 329  
to recent efforts trying to model and predict accurately the response of single neurons to 330  
complex stimuli in sensory areas [17, 47, 48]. 331

## Methods

332

**a Multi-electrode array recordings.** We analyze the response of rat RGCs to visual stimulation recorded in 9 multi-electrode array *ex-vivo* experiments [3], and spike sorted with *SpyKING CIRCUS* [49]. This dataset and the experimental methods have been already previously described [18]. In one experiment we probed the retinal response to three different visual stimuli: (i) a random black and white checkerboard, with spatio-temporal uncorrelated checkers; (ii) a full-field stimulus with fluctuating luminance and (iii) two gray horizontal bars performing an independent Brownian motion along the vertical direction [18]. In the other 8 experimental sessions, only the response to random black and white checkerboard and full-field was retained and analyzed here. Each of these stimulations lasted about 10sec and have been repeated at least  $R = 79$  times. Spiking times have been binned with a window of about 17ms, corresponding to a bin rate of 60Hz. With a custom algorithm [18]-similar to that of [7]- we used the cell's response to the full-field stimulation to identify the type of the recorded RGCs. Across the 9 experiments, we identified populations of  $20 \pm 6$  (mean  $\pm$  s.d.) OFF-Alpha cells.

333  
334  
335  
336  
337  
338  
339  
340  
341  
342  
343  
344  
345  
346

**b Stimulus and noise correlations.** After binning the spiking response of each cell, we estimate  $n_i^{(t,r)}$ , the number of emitted spikes by cell  $i$ , in the time-bin  $t$ , during repetition  $r$ , and its mean across repetitions  $\mu_i^{(t)}$ . Then we calculate the total covariance between two neurons  $(i, j)$  as follows:

347  
348  
349  
350

$$Cov_{total}(n_i, n_j) = \frac{1}{T} \sum_{t=1}^T \frac{1}{R} \sum_{r=1}^R (n_i^{(t,r)} - \mu_i)(n_j^{(t,r)} - \mu_j) \quad (1)$$

Where  $\mu_i = \sum_{t=1}^T \mu_i^{(t)} / T$  is the mean number of spikes across repetitions, and then averaged in time. It is possible to decompose the total covariance into a sum of the so called “stimulus” and “noise” covariances. We calculated these quantities as follows

351  
352  
353

$$Cov_{noise}(n_i, n_j) = \frac{1}{T} \sum_{t=1}^T \frac{1}{R} \sum_{r=1}^R (n_i^{(t,r)} - \mu_i^{(t)})(n_j^{(t,r)} - \mu_j^{(t)}) \quad (2)$$

354

$$Cov_{stimulus}(n_i, n_j) = \frac{1}{T} \sum_{t=1}^T \frac{1}{R} \sum_{r=1}^R (\mu_i^{(t)} - \mu_i)(\mu_j^{(t)} - \mu_j) \quad (3)$$

355

Noise correlations are then estimated as:

$$Corr_{noise}(n_i, n_j) = \frac{Cov_{noise}(n_i, n_j)}{\sqrt{V_i V_j}} \quad (4)$$

where  $V_i = Cov_{total}(n_i, n_i)$ .

356

Triplet noise correlations are instead defined as:

357

$$Corr_{noise}(n_i, n_j, n_k) = \frac{\frac{1}{T} \sum_{t=1}^T \frac{1}{R} \sum_{r=1}^R (n_i^{(t,r)} - \mu_i^{(t)})(n_j^{(t,r)} - \mu_j^{(t)})(n_k^{(t,r)} - \mu_k^{(t)})}{\sqrt{V_i V_j V_k}} \quad (5)$$

**c Copulas.** Copula-based modeling allows for disentangling the marginal distributions of two random variables from their mutual dependency, that can therefore be modeled alone, without the additional difficulties due to potentially complicated marginal distributions. Consider two random variables  $X$  and  $Y$ , with joint distribution  $f_{X,Y}$ , marginal distributions  $f_X$  and  $f_Y$  and marginal cumulative density function (c.d.f.)  $F_X$  and  $F_Y$  respectively. By construction, the random variables  $U_X \equiv F_X(X)$ ,  $X \sim f_X$  and  $U_Y \equiv F_Y(Y)$ ,  $Y \sim f_Y$  have uniform distributions over  $[0, 1]$ . Consequently the joint distribution of  $(U_X, U_Y)$  has uniform marginals, yet it contains all the information about the mutual dependence between  $X$  and  $Y$ . This property allows us to model the dependency of  $U_X$  and  $U_Y$  *instead* of that of  $X$  and  $Y$ . Specifically, a copula is the c.d.f. of the joint variable  $(U_X, U_Y)$ , i.e. a function  $C(\cdot, \cdot) : [0, 1]^2 \rightarrow [0, 1]$ . and it can be used to reconstruct the joint distribution of  $(X, Y)$ , via its c.d.f.:

$$F_{X,Y}(x, y) = C(F_X(x), F_Y(y)). \quad (6)$$

Sklar's theorem (see supplementary sect. S1) ensures the existence and uniqueness of  $C$ , and this allows for modeling the mutual dependency between  $X$  and  $Y$ , independently from their marginal distributions.

In most practical situations, the copula  $C$  is chosen from a parametric copula family. In this work we chose to work with Frank copulas:

$$C_{\text{Frank}}(u, v|\theta) = -\theta^{-1} \log \left( 1 + \frac{(e^{-\theta u} - 1)(e^{-\theta v} - 1)}{e^{-\theta} - 1} \right), \quad (7)$$

where  $\theta \in \mathcal{R}$  is the copula parameter, that can be estimated by log-likelihood maximization. We chose the Frank copula because this family has already been showed to perform well in modeling spike counts [35]. Once  $\theta$  has been inferred, the marginal distributions can in turn be approximated either with some model, or, as we will do in this work, empirically. We refer to the Mathematics section, the literature and textbooks (see, for example, [34]) for more explanations and details on copula models and/or other copula families.

**d Copula-based model.** We constructed a copula model able to predict  $P(n_i^{(t)}, n_j^{(t)})$ , the joint distribution of pair of spike counts in time:

$$P \left( \{n_i^{(t)}, n_j^{(t)}\}_{t=1}^T \right) = \prod_{t=1}^T c_{\text{Frank}} \left( F_i^{(t)}(n_i^{(t)}), F_j^{(t)}(n_j^{(t)}) \mid \hat{\theta}(d_{ij}) \right), \quad (8)$$

where  $c_{\text{Frank}}$  is the copula density function, corresponding to the c.d.f. of Eq. (7), and  $F_i^{(t)}(n_i^{(t)})$  is the *empirical* c.d.f.  $n_i^{(t)}$ , that we estimate across repetitions,  $d_{ij}$  is the distance between neurons  $i$  and  $j$ , and  $\hat{\theta}(d_{ij})$  is a parametric function:  $\hat{\theta}(d) = \exp(a + bd + cd^2)$  and  $\hat{\theta}(d) = 0$  if  $d > 1\text{mm}$ . To infer this function from data, we first inferred a copula parameter for each pair of neurons,  $\theta_{ij}$ , by log-likelihood maximization, and then we obtained  $a = 3.2, b = -0.013\mu\text{m}^{-1}$  and  $c = 7 \cdot 10^{-6}\mu\text{m}^{-2}$  by fitting the behavior of  $\theta_{ij}$  with respect to the distance  $d_{ij}$ . See supplementary sect. S2 for further information.



**e Time-dependent Maximum Entropy model.** The time-dependent maximum entropy model we used is: 390  
391

$$P\left(\left\{\{n_i^{(t)}\}_{i=1}^N\right\}_{t=1}^T\right) = \prod_{t=1}^T \left( \exp \left\{ \sum_i h_i^{(t)} n_i^{(t)} + \sum_{i \leq j} n_i^{(t)} J_{ij} n_j^{(t)} - \sum_i \ln(n_i^{(t)}!) \right\} / Z^{(t)} \right) \quad (9)$$

where  $n_i^{(t)} \in [0, 1, \dots, n^{\text{Max}}]$  is an integer spike-count, with  $n^{\text{Max}}$  matched from data. The index “ $(t)$ ” expresses the time dependence.  $Z^{(t)}$  is a normalization constant (the partition function).  $h_i^{(t)}$  is the local field for neuron  $i$  at time  $t$  imposing the firing probability and  $J_{ij}$  is the couplings network that allows for reproducing the system’s correlations. Note that  $J_{ij}$  does not depend on time and it includes also the diagonal terms  $J_{ii}$  which set each neurons variance equal to its empirical value [33, 50]. The log-factorial term allows for matching the single neurons statistics [50], as by taking  $J = 0$  the model reduces to a collection of independent Poisson distributions. 392  
393  
394  
395  
396  
397  
398  
399

The inference of the model (9) is done by log-likelihood maximization using an iterative algorithm with adaptive learning rate similar to that of [51]. Thanks to its exponential form, the model inference requires only the average value of  $n_i^{(t)}$  across repetitions and the value of the noise covariances (see Methods). In our case we estimate the first from the marginal response of each neurons and we used the copula model to predict the second. 400  
401  
402  
403  
404

**f Synthetic lattice.** In order to construct a synthetic lattice that respects the inter-cells distance of empirical recordings, we started by a triangular regular lattice with side  $194\mu m$ , and then we added a Gaussian noise with a standard deviation of  $22\mu m$  to the x and y coordinate of each cells. These parameters are optimized in order to match the distribution of cells distances measured in real experimental recordings. 405  
406  
407  
408  
409

**g Population activity variance and synchrony.** In this paper we compute the population activity as the sum of all spike-counts,  $\sum_i n_i(t)$ . To compute the “population activity variance” of Fig. 5C we first estimate the variance of the population activity for each time-bin. Then we averaged over time and finally we normalized by the population size. “Synchrony” of Fig. 5D is instead the probability of observing an event with a population activity larger than the mean plus one standard deviation of the population activity of the shuffled model. We compute this for each time-bin and then we averaged over time. 410  
411  
412  
413  
414  
415  
416

## S1. Supplementary mathematics

417

**a Copula’s definition.** A copula function is the c.d.f. of a bi-variate distribution with  $Uniform(0, 1)$  marginals. This mathematical construct allows to model the dependency structure of bi-variate random variables separately from their marginal distributions, as the following theorem shows.

418  
419  
420  
421

**b Sklar’s theorem.** Let  $X$  and  $Y$  be any two, mutually dependent, real random variables. Let  $F_X$ ,  $F_Y$ , and  $F_{(X,Y)}$  be the c.d.f.s of  $X$ ,  $Y$ , and  $(X, Y)$  respectively. Note that for any  $X$  we have  $F_X(X) \equiv Uniform(0, 1)$ , *idem* for  $Y$ . The Sklar theorem asserts that given such  $X$ , and  $Y$ :

422  
423  
424  
425

$$\exists! \text{ a copula } C, \text{ such that } F_{X,Y}(x, y) = C(F_X(x), F_Y(y)) \quad (10)$$

**c Discrete copulas.** The proof of existence of Sklar’s theorem holds for both continuous, and discrete random variables (as is our case). However, in practice, to apply copula models in the discrete case we need to make adjustments. In particular we turn a continuous copula, into a discrete distribution that may take values in a countable set of points in  $[0, 1]$ . By doing so we define a so called “pseudo density” function, that describes a discrete counterpart to copulas. Assuming that  $(X, Y) \in \mathcal{N}^2$ , without loss of generality, the “pseudo density” of a copula defined by a copula density  $c$  is given by:

426  
427  
428  
429  
430  
431  
432

$$f_{pseudo}(F_X(x), F_Y(y)) = \int_{F_X(x-1)}^{F_X(x)} \int_{F_Y(y-1)}^{F_Y(y)} c(u, v) du dv \quad (11)$$

## S2. Supplementary information: model construction

433

Here we fully justify how we simplified the copula model, from its bare version with one parameter for each neuron pair in each time-bin, to the final version with just three parameters in total.

434  
435  
436

As explained in the Methods section, our starting point is a copula model where for each neuron pair  $(i, j)$  and each time-bin  $t$  a copula parameter  $\theta_{ij}^{(t)}$  accounts for the correlation between the two spike-counts. Despite being very accurate, this model has little capacities to generalize across stimulus conditions or experiments. Moreover, because of the large number of parameters is potentially pruned to overfitting. In Fig. S1A, for an example neuron pair, we show the values of the inferred parameters in all time-bins plotted against the mean firing rate of the two cells -in the corresponding time-bin and computed across repetitions. As can be observed, at high firing rate, that is when the statistics is large and the inference error is small, the inferred parameters tend to accumulate around a single value. This result suggested us that a model where the copula parameters does not depend on time could have a similar performance, yet requiring much less parameters.

437  
438  
439  
440  
441  
442  
443  
444  
445  
446  
447

In order to infer such time-independent copula parameters, for each neuron pair, we first select the “active” time-bins where the two neurons spiked synchronously in at least one repetition:  $\sum_{r=1}^R n_{i,r}^t n_{j,r}^t > 0$ , where  $n_{i,r}^t$  is the number of spikes emitted by neuron  $i \in [1, \dots, N]$ , in time bin  $t \in [1, \dots, T]$  during repetition  $r \in [1, \dots, R]$ . Once the inactive time bins are filtered out, we estimate the model parameter by maximizing the likelihood:

448  
449  
450  
451  
452

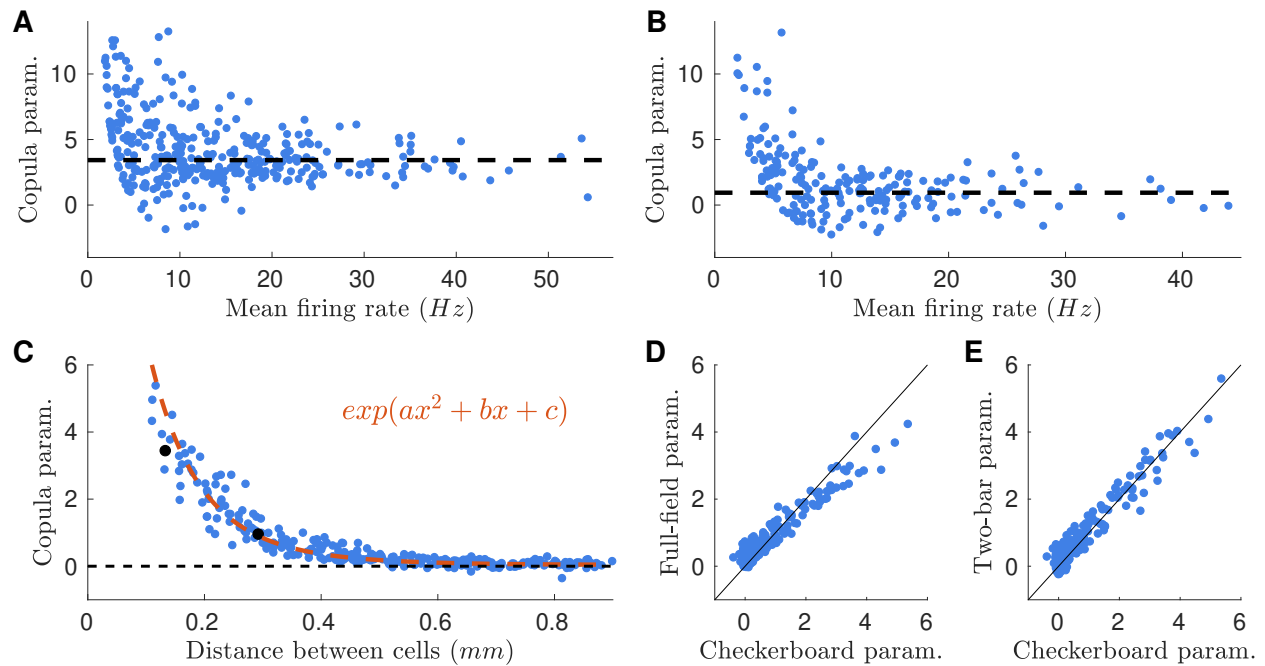


**FIG. S1: Stimulus-conditioned copula model is robust across different stimulus ensembles.** **A)** Values of the inferred copula parameter in all time-bins for an example neuron pair, plotted against the mean firing rate of the two cells. Horizontal line correspond to the inferred parameter in the *time-independent* copula model (see text) **B)** As **A**, but for another example pair. **C)** Inferred Frank copula's parameters plotted against the distance between cells for checkerboard stimulation. Parameters of each pairs are inferred independently. Orange: exponential fit used for estimating the copula parameter from the cell distance in the final version of the model. **D)** Scatterplot of the *time-independent* (see text) parameters inferred from checkerboard and full-field stimulations **E)** Scatterplot of the parameters inferred from checkerboard and two-bar stimulations

$$l(\theta|X) = \sum_t \sum_{r=1}^R \log(f_{pseudo}^{(t)}(n_{i,r}^{(t)}, n_{j,r}^{(t)}|\theta)) = \sum_t \sum_{r=1}^R \log \int_{F_i^{(t)}(n_{i,r}^{(t)}-1)}^{F_i^{(t)}(n_{i,r}^{(t)})} \int_{F_j^{(t)}(n_{j,r}^{(t)}-1)}^{F_j^{(t)}(n_{j,r}^{(t)})} c_\theta(u, v) du dv \quad (12)$$

where the summation over  $t$  runs over the active time-bins for the neuron pair. Note how  $F$ , and thus  $f_{pseudo}$ , depends on  $t$ , as the empirical marginals are estimated separately for every time bin. We infer the time-independent copula parameters  $\theta_{ij}$  by log-likelihood maximization for each neurons' pair and for checkerboard, full-field and two-bar stimuli. Figs. S1B and C compare the parameters inferred from different stimuli and show how the inference is robust across changes of visual stimulation. The copula parameter thus reflect some properties of the retinal network, independent of the current stimulus ensemble.

Fig. S1C show the behavior of the inferred checkerboard parameters with respect to the physical distance between cells. Furthermore these parameters are independent of the visual stimulus (see Figs. S1D and E). These results suggested us that a simple fit of copula parameters may account for most of the variability of the parameter values across neuron

pairs.

To further simplify our copula model, and reduce the number of its parameters, we hence fitted the inferred copula parameters with a parametric function of the inter-cell distance  $d$ :  $\theta(d) = \exp(a + bd + cd^2)$ . The copula model takes now as input only the distance between the cells, uses it to estimate the copula parameter, and then construct the joint spike-count distribution using Eq. (8).

### S3. Supplementary information: simplest model for noise correlations

In this section we compare the performance of our copula-based approach in predicting noise correlations with a straightforward model that assumes distant-dependent noise correlations.

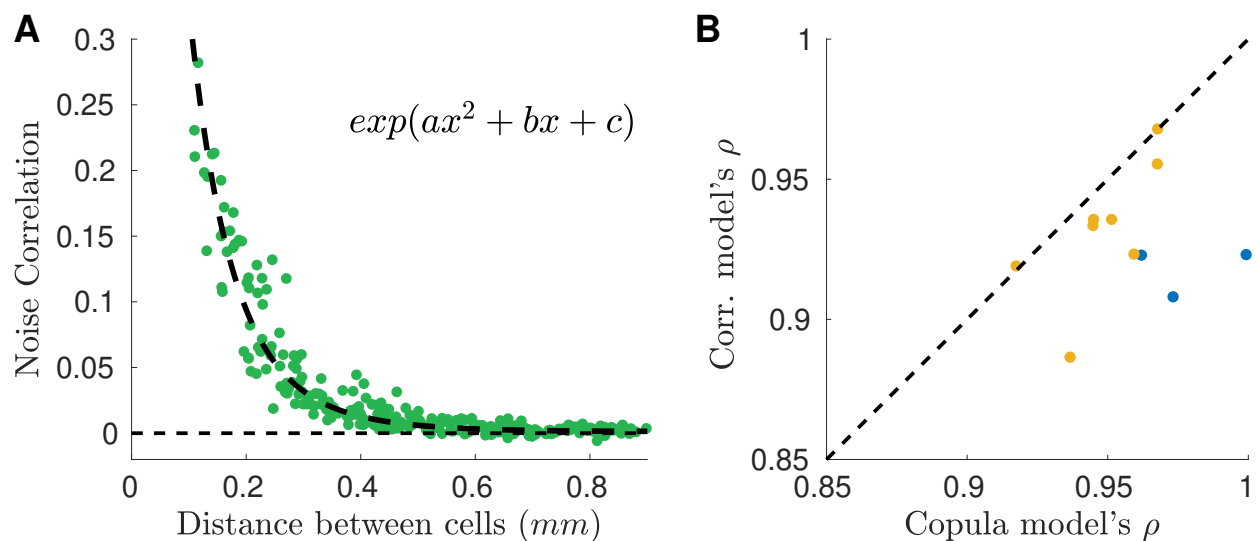


**FIG. S2: Copula model outperforms simpler model with distant dependent noise-correlations.** **A)** Construction of the model: noise correlations observed in one experiment (Exp. #1) are fitted with an exponential function of the distance between neurons. Such fit is then used to predict noise correlations in other experiments. **B)** Performance in predicting noise correlation for our copula model against the model presented here. Blue points: performance for the first dataset with three different stimulus ensembles. Yellow points: performance for the other experimental sessions.

Noise correlations decrease with the distance between the corresponding neurons (see Fig. 1 and Fig. S2A). We fit this relation with an exponential function, and we asked to what extent this behavior is conserved across experiments. To estimate this, we used this simple method to predict noise correlations in all the experiments described before. Although the predictions were accurate, our copula model outperforms this simpler approach (see Fig. S2B).

## Acknowledgments

480

We like to thank M. Chalk and G. Tkacik for useful discussions. This work was supported by ANR Trajectory, the French State program Investissements d'Avenir managed by the Agence Nationale de la Recherche (LIFESENSES; ANR-10-LABX-65), EC Grant No. H2020-785907 from the Human Brain Project, NIH Grant No. U01NS090501, and an AVIESAN-UNADEV grant to O.M.

481

482

483

484

485

- 
- [1] G. Buzáki. *Large-scale recording of neuronal ensembles*. Nat Neurosci. , **7(5)**:446–51, 2004.
  - [2] Adam M Packer, Lloyd E Russell, Henry WP Dalgleish, and Michael Häusser. Simultaneous all-optical manipulation and recording of neural circuit activity with cellular resolution in vivo. *Nature methods*, 12(2):140, 2014.
  - [3] O. Marre, D. Amodei, N. Deshmukh, K. Sadeghi, F. Soo, T. Holy, and M.J. Berry. *Recording of a large and complete population in the retina*. Journal of Neuroscience , **32(43)**:1485973, 2012.
  - [4] Diwakar Turaga and Timothy E Holy. Organization of vomeronasal sensory coding revealed by fast volumetric calcium imaging. *Journal of Neuroscience*, 32(5):1612–1621, 2012.
  - [5] Anna L Vlasits, Thomas Euler, and Katrin Franke. Function first: classifying cell types and circuits of the retina. *Current opinion in neurobiology*, 56:8–15, 2019.
  - [6] Karl Farrow and Richard H Masland. Physiological clustering of visual channels in the mouse retina. *American Journal of Physiology-Heart and Circulatory Physiology*, 2011.
  - [7] T. Baden, P. Berens, K. Franke, M.R. Rosn, M. Bethge, and T. Euler. *The functional diversity of retinal ganglion cells in the mouse*. Nature , **529**:345–50, 2016.
  - [8] G.L.B. Spampinato, E. Ronzitti, V. Zampini, U. Ferrari, F. Trapani, H. Khabou, D. Dalkara, S. Picaud, E. Papagiakoumou, O. Marre, and V. Emiliani. All-optical interrogation of a direction selective retinal circuit by holographic wave front shaping. *bioRxiv*, page 513192, 2019.
  - [9] Michael N Economo, Sarada Viswanathan, Bosiljka Tasic, Erhan Bas, Johan Winnubst, Vilas Menon, Lucas T Graybuck, Thuc Nghi Nguyen, Kimberly A Smith, Zizhen Yao, et al. Distinct descending motor cortex pathways and their roles in movement. *Nature*, 563(7729):79, 2018.
  - [10] Mean-Hwan Kim, Petr Znamenskiy, Maria Florencia Iacaruso, and Thomas D Mrsic-Flogel. Segregated subnetworks of intracortical projection neurons in primary visual cortex. *Neuron*, 100(6):1313–1321, 2018.
  - [11] Rava Azeredo da Silveira and Botond Roska. Cell types, circuits, computation. *Current opinion in neurobiology*, 21(5):664–671, 2011.
  - [12] Karthik Shekhar, Sylvain W Lapan, Irene E Whitney, Nicholas M Tran, Evan Z Macosko, Monika Kowalczyk, Xian Adiconis, Joshua Z Levin, James Nemeshe, Melissa Goldman, et al. Comprehensive classification of retinal bipolar neurons by single-cell transcriptomics. *Cell*, 166(5):1308–1323, 2016.
  - [13] Xiaolong Jiang, Shan Shen, Cathryn R Cadwell, Philipp Berens, Fabian Sinz, Alexander S Ecker, Saumil Patel, and Andreas S Tolias. Principles of connectivity among morphologically defined cell types in adult neocortex. *Science*, 350(6264):aac9462, 2015.

- [14] E.J. Chichilnisky. A simple white noise analysis of neuronal light responses. *Network: Computation in Neural Systems*, 12(2):199–213, 2001.
- [15] J.W. Pillow, J. Shlens, L. Paninski, A. Sher, A.M. Litke, E. J. Chichilnisky, and E.P. Simoncelli. *Spatio-temporal correlations and visual signalling in a complete neuronal population*. *Nature*, 454:995–999, 2008.
- [16] J.M. McFarland, Y. Cui, and D.A. Butts. Inferring nonlinear neuronal computation based on physiologically plausible inputs. *PLoS Comput Biol*, 9(7):e1003143, 2013.
- [17] L. McIntosh, N. Maheswaranathan, A. Nayebi, S. Ganguli, and S. Baccus. Deep learning models of the retinal response to natural scenes. In *Advances in Neural Information Processing Systems*, pages 1361–1369, 2016.
- [18] S. Deny, U. Ferrari, E. Mace, P. Yger, R. Caplette, S. Picaud, G. Tkačik, and O. Marre. Multiplexed computations in retinal ganglion cells of a single type. *Nature communications*, 8(1):1964, 2017.
- [19] AMHJ Aertsen, Peter IM Johannesma, and DJ Hermes. Spectro-temporal receptive fields of auditory neurons in the grassfrog. *Biological Cybernetics*, 38(4):235–248, 1980.
- [20] Maneesh Sahani and Jennifer F Linden. How linear are auditory cortical responses? In *Advances in neural information processing systems*, pages 125–132, 2003.
- [21] Stephen V David, William E Vinje, and Jack L Gallant. Natural stimulus statistics alter the receptive field structure of v1 neurons. *Journal of Neuroscience*, 24(31):6991–7006, 2004.
- [22] Thomas A Münch, Rava Azeredo Da Silveira, Sandra Siegert, Tim James Viney, Gautam B Awatramani, and Botond Roska. Approach sensitivity in the retina processed by a multifunctional neural circuit. *Nature neuroscience*, 12(10):1308, 2009.
- [23] E. Schneidman, W. Bialek, and M.J. Berry. Synergy, redundancy, and independence in population codes. *Journal of Neuroscience*, 23(37):11539–11553, 2003.
- [24] P. K. Trong and F. Rieke. Origin of correlated activity between parasol retinal ganglion cells. *Nature neuroscience*, 11(11):1343–1351, 2008.
- [25] J. Shlens, F. Rieke, and E.J. Chichilnisky. Synchronized firing in the retina. *Current opinion in neurobiology*, 18(4):396–402, 2008.
- [26] M. Greschner, J. Shlens, C. Bakolitsa, G.D. Field, J. L. Gauthier, L. H Jepson, A. Sher, A. M. Litke, and E.J. Chichilnisky. Correlated firing among major ganglion cell types in primate retina. *The Journal of Physiology*, 589(1):75–86, 2011.
- [27] Dmitry R Lyamzin, Samuel J Barnes, Roberta Donato, Jose A Garcia-Lazaro, Tara Keck, and Nicholas A Lesica. Nonlinear transfer of signal and noise correlations in cortical networks. *Journal of Neuroscience*, 35(21):8065–8080, 2015.
- [28] X. Pitkow and M. Meister. Decorrelation and efficient coding by retinal ganglion cells. *Nat. Neurosci.*, 15(4):628–635, 2012.
- [29] F. Franke, M. Fiscella, M. Sevelev, B. Roska, A. Hierlemann, and R.A. da Silveira. Structures of neural correlation and how they favor coding. *Neuron*, 89(2):409–422, 2016.
- [30] E. Schneidman, M. Berry, R. Segev, and W. Bialek. *Weak pairwise correlations imply strongly correlated network states in a population*. *Nature*, 440:1007, 2006.
- [31] Hideaki Shimazaki, Shun-ichi Amari, Emery N Brown, and Sonja Grün. State-space analysis of time-varying higher-order spike correlation for multiple neural spike train data. *PLoS computational biology*, 8(3):e1002385, 2012.
- [32] E. Granot-Atedgi, G. Tkacik, R. Segev, and E. Schneidman. Stimulus-dependent maximum entropy models of neural population codes. *PLOS Computational Biology*, 9(3):1–14, 2013.

- [33] U. Ferrari, S. Deny, M. Chalk, G. Tkačik, O. Marre, and T. Mora. Separating intrinsic interactions from extrinsic correlations in a network of sensory neurons. *Physical Review E*, 98(4):042410, 2018.
- [34] Pravin K Trivedi, David M Zimmer, et al. Copula modeling: an introduction for practitioners. *Foundations and Trends® in Econometrics*, 1(1):1–111, 2007.
- [35] Pietro Berkes, Frank Wood, and Jonathan W Pillow. Characterizing neural dependencies with copula models. In *Advances in neural information processing systems*, pages 129–136, 2009.
- [36] Arno Onken, Steffen Grünewälder, Matthias HJ Munk, and Klaus Obermayer. Analyzing short-term noise dependencies of spike-counts in macaque prefrontal cortex using copulas and the flashlight transformation. *PLoS computational biology*, 5(11):e1000577, 2009.
- [37] Houman Safaai, Arno Onken, Christopher D Harvey, and Stefano Panzeri. Information estimation using nonparametric copulas. *Physical Review E*, 98(5):053302, 2018.
- [38] S. Cocco, S. Leibler, and R. Monasson. *Neuronal couplings between retinal ganglion cells inferred by efficient inverse statistical physics methods*. Proc. Natl. Acad. Sci. USA , **106**:14058, 2009.
- [39] Stewart A Bloomfield and Béla Völgyi. The diverse functional roles and regulation of neuronal gap junctions in the retina. *Nature Reviews Neuroscience*, 10(7):495, 2009.
- [40] P. Ala-Laurila, M. Greschner, E.J. Chichilnisky, and F. Rieke. Cone photoreceptor contributions to noise and correlations in the retinal output. *Nature neuroscience*, 14(10):1309–1316, 2011.
- [41] Laura Sacerdote, Massimiliano Tamborrino, and Cristina Zucca. Detecting dependencies between spike trains of pairs of neurons through copulas. *Brain research*, 1434:243–256, 2012.
- [42] Arno Onken and Stefano Panzeri. Mixed vine copulas as joint models of spike counts and local field potentials. In *Advances in Neural Information Processing Systems*, pages 1325–1333, 2016.
- [43] Siwei Wang, Alexander Borst, Noga Zaslavsky, Naftali Tishby, and Idan Segev. Efficient encoding of motion is mediated by gap junctions in the fly visual system. *PLoS computational biology*, 13(12):e1005846, 2017.
- [44] G. Tkacik, O. Marre, D. Amodè, E. Schneidman, W Bialek, and Berry M.J. *Searching for collective behaviour in a network of real neurons*. PloS Comput. Biol., **10**(1):e1003408, 2014.
- [45] Marcel Nonnenmacher, Christian Behrens, Philipp Berens, Matthias Bethge, and Jakob H Macke. Signatures of criticality arise from random subsampling in simple population models. *PLoS Computational Biology*, 13(10):e1005718, 2017.
- [46] Mihály Bányai, Andreea Lazar, Liane Klein, Johanna Klon-Lipok, Marcell Stippinger, Wolf Singer, and Gergő Orbán. Stimulus complexity shapes response correlations in primary visual cortex. *Proceedings of the National Academy of Sciences*, page 201816766, 2019.
- [47] Santiago A Cadena, George H Denfield, Edgar Y Walker, Leon A Gatys, Andreas S Tolia, Matthias Bethge, and Alexander S Ecker. Deep convolutional models improve predictions of macaque v1 responses to natural images. *BioRxiv*, page 201764, 2018.
- [48] D.L.K. Yamins and J.J. DiCarlo. Using goal-driven deep learning models to understand sensory cortex. *Nature neuroscience*, 19(3):356–365, 2016.
- [49] Pierre Yger, Giulia LB Spampinato, Elric Esposito, Baptiste Lefebvre, Stéphane Deny, Christophe Gardella, Marcel Stimberg, Florian Jetter, Guenther Zeck, Serge Picaud, et al. A spike sorting toolbox for up to thousands of electrodes validated with ground truth recordings in vitro and in vivo. *ELife*, 7:e34518, 2018.

- [50] U Ferrari, S. Deny, O Marre, and T Mora. A simple model for low variability in neural spike trains. *Neural Computation*, 30(11), 2018.
- [51] U. Ferrari. Learning maximum entropy models from finite-size data sets: A fast data-driven algorithm allows sampling from the posterior distribution. *Phys. Rev. E*, 94:023301, 2016.